Journal of Physiology (2002), **539.3**, *pp.* 681–691
DOI: 10.1013/jphysiol.2001.013246

www.jphysiol.org

α_{1H} mRNA in single skeletal muscle fibres accounts for T-type calcium current transient expression during fetal development in mice

Christine Berthier *, Arnaud Monteil †, Philippe Lory † and Caroline Strube *

* *CNRS-UMR 5123, UCB-Lyon 1, 69622 Villeurbanne and † IGH, CNRS-UPR 1142, 34396 Montpellier, France*

Calcium channels are essential for excitation–contraction coupling and muscle development. At the end of fetal life, two types of Ca^{2+} currents can be recorded in muscle cells. Whereas L-type Ca^{2+} channels have been extensively studied, T-type channels have been poorly characterized in skeletal muscle. We describe here the functional and molecular properties of T-type calcium channels in developing mouse skeletal muscle. The T-type current density increased transiently during prenatal myogenesis with a maximum at embryonic day E16 followed by a drastic decrease until birth. This current showed similar electrophysiological and pharmacological properties at all examined stages. It displayed a wide window current centred at about −35 and −55 mV in 10 and 2 mM external Ca^{2+}, respectively. Activation and inactivation kinetics were fast (3 and 16 ms, respectively). The current was inhibited by nickel and amiloride with an IC_{50} of 5.4 and 156 μM, respectively, values similar to those described for cloned T-type α_{1H} channels. Whole muscle tissue RT-PCR analysis revealed mRNAs corresponding to α_{1H} and α_{1G} subunits in the fetus but not in the adult. However, single-fibre RT-PCR demonstrated that only α_{1H} mRNA was present in prenatal fibres, suggesting that the α_{1G} transcript present in muscle tissue must be expressed by non-skeletal muscle cells. Altogether, these results demonstrate that the α_{1H} subunit generates functional T-type calcium channels in developing skeletal muscle fibres and suggest that these channels are involved in the early stages of muscle differentiation.

(Received 6 September 2001; accepted after revision 3 December 2001)
Corresponding author C. Strube: UMR CNRS 5123, Bat R. Dubois, 43 Bd du 11 novembre 1918, 69622 Villeurbanne Cedex, France. Email: caroline.strube@univ-lyon1.fr

Calcium ions and voltage-dependent Ca^{2+} channels are essential in skeletal muscle function, particularly for excitation–contraction coupling (for review see Catterall, 1991; Melzer *et al.* 1995). Calcium influx is also required for muscle development and has been shown to be involved in several steps including phenotypic differentiation (Shainberg *et al.* 1969; Morris & Cole, 1979; Salzberg *et al.* 1995) and myoblast fusion (Seigneurin-Venin *et al.* 1996; Bijlenga *et al.* 2000). Prenatal myogenesis involves the fusion of embryonic and fetal myoblasts to form multi-nucleated primary and secondary myofibres that will further differentiate into adult muscle fibres (Miller *et al.* 1999). At the end of fetal life, two types of Ca^{2+} currents can be recorded in myofibres: L-type, high voltage activated (HVA) Ca^{2+} currents and T-type, low voltage activated (LVA) Ca^{2+} currents (Beam & Knudson, 1988*a*; Shimahara & Bournaud, 1991; Strube *et al.* 2000). Whereas L-type Ca^{2+} channels have been extensively studied during the past decade, the absence of a pharmacological agent specific for T-type Ca^{2+} channels has hampered the understanding of their physiological function. T-type currents were first described in starfish eggs by Hagiwara *et al.* in 1975. It then took almost 10 years to record them from vertebrates in sensory neurons (Carbone & Lux, 1984; Bossu *et al.* 1985; Nowycky *et al.* 1985), pituitary cells (Matteson & Armstrong, 1986) and cardiomyocytes (Nilius *et al.* 1985). Their properties include fast inactivation kinetics, activation just above resting potential, slow deactivation and a small unitary conductance. In skeletal muscle, T-type currents described in primary culture (Cognard *et al.* 1986) and in freshly isolated embryonic fibres (Shimahara & Bournaud, 1991; Strube *et al.* 2000) disappear 3–4 weeks after birth (Beam & Knudson, 1988*b*), suggesting that they could be involved in some developmental process.

The recent molecular identification of a novel family of genes encoding T-type Ca^{2+} channel α_1 subunits, has provided new tools to probe their physiological functions. Three genes, CACNA1G, CACNA1H and CACNA1I encoding the α_{1G} ($Ca_V3.1$) subunit (Perez-Reyes *et al.* 1998; Monteil *et al.* 2000*a*), the α_{1H} ($Ca_V3.2$) subunit (Cribbs *et al.* 1998; Williams *et al.* 1999) and the α_{1I} ($Ca_V3.3$) subunit (Lee *et al.* 1999*a*; Monteil *et al.* 2000*b*), respectively, have been identified. When expressed in HEK 293 cells these subunits generate currents with the typical hallmarks of native T-type channels. However, the

gating behaviour of α_{1I} channels is distinct, activating and inactivating 5- to 10-fold slower than either α_{1G} or α_{1H} channels (Klöckner *et al.* 1999; Kozlov *et al.* 1999; Monteil *et al.* 2000*b*). Moreover, the recovery of α_{1H} from short-term inactivation is more than 3-fold slower than for α_{1G} or α_{1I} (Klöckner *et al.* 1999; Kozlov *et al.* 1999). Finally, the T-type current induced by α_{1H} is 10 to 20 times more sensitive to nickel ions than those induced by either α_{1G} or α_{1I} (Lee *et al.* 1999*b*), and the α_{1H} current is more than 50 times more sensitive to amiloride than the α_{1G} current (Williams *et al.* 1999; Lacinova *et al.* 2000*a*). Taking advantage of the molecular blueprint of these channel isoforms, we have used electrophysiological and RT-PCR techniques to characterize the functional expression of the various T-type channel α_1 subunits during development in mouse skeletal muscle.

METHODS

Single cell preparation

All experiments were performed on freshly isolated intercostal myofibres from 14- to 18-day-old mouse fetuses. Mice (Swiss OF1 from IFFA CREDO, l'Arbresle, France) were mated overnight. The ages of fetuses were determined by defining embryonic day 0 (E0) as that of the appearance of the vaginal plug in the morning. Pregnant mice were killed by cervical dislocation and the fetuses by decapitation, in accordance with local ethical guidelines. The two halves of the ribcage of each fetus were dissected in normal Tyrode solution containing (mM): 140 NaCl, 5 KCl, 2.5 $CaCl_2$, 1 $MgCl_2$, 10 Hepes–NaOH, pH 7.4. The tissues were incubated at 37 °C for 5–12 min in phosphate-buffered saline (Sigma, Saint Quentin Fallavier, France), containing 3 mg ml^{-1} collagenase (type I, Sigma) and 1 mg ml^{-1} trypsin (type III, Sigma). Cells were then mechanically dispersed and collected in plastic Petri dishes (35 mm diameter) containing Tyrode solution. Cells were maintained for at least 1 h at room temperature in Tyrode solution before the electrophysiological experiments.

Ca^{2+} current recordings

The standard patch-clamp technique was used in the whole-cell recording configuration. The external solution was (mM): 130 TEA methanesulphonate, 10 $CaCl_2$, 1 $MgCl_2$, 10^{-3} TTX, 10 Hepes–TEA(OH), pH 7.4. The pipette solution consisted of (mM): 140 caesium aspartate, 1 $MgCl_2$, 10 EGTA, 10 Mops–CsOH, pH 7.2. Recordings were made with a RK 400 patch clamp amplifier (Bio-Logic, Claix, France) at room temperature. The effective series resistance was analogically compensated close to the point of amplifier oscillation. Cell capacitance was determined by integration of a capacity transient elicited by a −10 mV hyperpolarizing pulse from a holding potential of −80 mV and was used to compute the Ca^{2+} current density of each cell as previously described (Strube *et al.* 1996). The voltage drop due to series resistance ($R_s \times I_{max}$) was measured for each cell and never exceeded 2.4 mV. The average value was 0.96 ± 0.08 mV ($n = 54$). The average time constant to charge the membrane capacitance ($R_s \times C_m$) was 0.35 ± 0.02 ms ($n = 54$) and never exceeded 0.86 ms. Data acquisition and command voltage pulse generation were performed with a Digidata 1200 interface controlled by pCLAMP6 software (Axon Instruments, Foster City, CA, USA). Data were filtered at 0.3–1 kHz and digitized at 1–2 kHz. Data were analysed using pCLAMP6 and Sigmaplot (Jandel, San Rafael, CA, USA) software packages. Results are presented as means ± S.E.M. and n is the number of cells.

Activation and inactivation analysis

As previously described (Strube *et al.* 2000), the voltage dependence of the Ca^{2+} current density curves was fitted according to eqn (1):

$$I(V) = G_{max}(V - V_{rev})/(1 + \exp[(V_{½,ac} - V)/k_{ac}]), \quad (1)$$

where $I(V)$ is the peak density of current in response to the test depolarizing potential V, V_{rev} is the apparent reversal potential (determined as one of the fitted parameters), G_{max} is the maximum conductance for the peak current, $V_{½,ac}$ is the potential that elicits the half-maximum increase in conductance, and k_{ac} is a steepness parameter. For each cell, the values of G_{max} and V_{rev} calculated from the fit were used to estimate the voltage dependence of the activation (normalized conductance) using eqn (2):

$$G(V)/G_{max} = I(V)/(G_{max}(V - V_{rev})). \quad (2)$$

The voltage dependence of the inactivation was studied using a double pulse protocol. To compare this property at different developmental stages, a 300 ms conditioning pulse of variable amplitude (reaching between −80 and +20 mV in 5 mV steps) from a holding potential of −80 mV was separated from a fixed test pulse of 100 ms duration to −20 mV by a short pulse of 5 ms to −80 mV. The amplitude of the current elicited by the test pulse was normalized with respect to the control current obtained with the conditioning pulse to −80 mV and plotted *versus* the potential reached by the conditioning pulse. A Boltzmann fit of the values allows the calculation of $V_{½,inac}$ which is the potential that elicits the half-maximum inactivation, and k_{inac} which is a steepness parameter. To evaluate at best the window current component of the current in physiological Ca^{2+} concentration, steady-state inactivation property was studied using a 10 s conditioning pulse.

The time courses of the macroscopic T-type Ca^{2+} current densities were fitted by the sum of two exponential components (eqn (3)) as used by others (Kozlov *et al.* 1999; Lee *et al.* 1999*a*):

$$I(t) = A_1 \times \exp(-t/\tau_1) + A_2 \times \exp(-t/\tau_2) + C, \quad (3)$$

where $I(t)$ is the current density at time t after the depolarization, τ_1 and τ_2 are the time constants for the two components of the current time course, C is the steady state current, and A_1 and A_2 are the amplitudes for each component.

Dose–response analysis

To make the $NiCl_2$ solution, a 200 mM $NiCl_2$ stock solution in deionized water was diluted on the day of the experiment by at least 1:400 in the external solution. To make the amiloride solution, a 1 M amiloride (Sigma) stock solution in DMSO was also diluted on the day of the experiment by at least 1:200 in the external solution. The stock solutions were stored at 4 °C. After the establishment of the whole-cell configuration, cells were continuously perfused by either control solution or different test solutions throughout the recording. The test solutions were applied in a cumulative manner starting from the lowest to the highest antagonist concentration and back to the control solution at the end of the experiment. A dose–response curve was fitted with a simple binding function of the form (eqn (4)):

$$I/I_{max} = 1/(1 + ([\text{antagonist}]/IC_{50})^{n_H}), \quad (4)$$

where I is the amplitude of the current at a given antagonist concentration, I_{max} is the amplitude of the current in control

condition (in the absence of drug), IC_{50} the concentration at which half the current was blocked and n_H the Hill coefficient.

RT-PCR on whole tissue extracts

Skeletal muscle tissues were collected from hindlimbs at various embryonic (E) and postnatal (P) stages and frozen immediately in liquid nitrogen. Total RNA was extracted according to the method of Chomczynski & Sacchi (1987). RNA was treated with DNAse (Promega Corp., Madison, WI, USA) according to the manufacturer's instructions. First strand cDNA synthesis (reverse transcription, RT) was carried out in a 25 μl reaction in the presence of RNAse inhibitor (RNaseOUT, Life technologies Inc., Rockville, MD, USA) using Sensiscript reverse transcriptase (Qiagen SA, Courtaboeuf, France) and 0.8 μM of sequence-specific primer for the domain III (between S3 and S4 segments) of the α_{1G}, α_{1H} and α_{1I} transcripts:

5′-ATGATRCGGATGATGGTGG-3′.

Control reverse transcription reactions were performed in the absence of reverse transcriptase (not shown). RT-PCR amplification was performed according to standard protocols using sets of specific forward and reverse primers:

for α_{1G}: 5′-CCACCTCTCATCATCCACAC-3′,
and 5′-CCCTCATCATCGCCATCATC-3′.
α_{1H}: 5′-TGAGGATAAGACATCTACCCAC-3′
and 5′-TGACTTTCTGGCAGGAGAC-3′.
α_{1I}: 5′-ATGCTGGTGATCCTGCTGAAC-3′
and 5′-GCACGCGGTTGATGGCTTTGAG-3′.

Control experiments were performed on brain RNA extract (positive control) as well as by omitting cDNA during amplification (H_2O negative control). G3PDH amplification was performed on oligo-dT primed RT products.

Single-fibre RT-PCR. RT-PCR was performed according to Lambolez *et al.* (1992) with some modifications. Experiments were carried out using whole fibres freshly isolated from ribcages of 18-day-old mouse fetuses. Harvest of intracellular content alone proved unfeasible under our conditions, owing probably to the high density of the cytoskeleton-rich cytoplasm of these cells. Enzymatically dissociated fibres were filtered on 50 μm mesh nylon filters and rinsed 8–10 times with Tyrode solution, in order to eliminate non-muscle cells and cellular fragments. Cells in Tyrode solution were then aspirated through Teflon tubing under microscopic control. One single fibre was collected in a final volume of 5 μl and immediately transferred to a prechilled microfuge tube containing RT solution: 5 μM random hexamers (Life technologies), 0.5 mM of each dNTP (Amersham), RT buffer (Life technologies), 2 units μl^{-1} RNAse inhibitor (Life technologies) and 10 mM DTT. Fibres were broken open by two freeze–thaw cycles. For cDNA synthesis, 100 units of Mohoney murine Leukaemia virus (MMLV) reverse transcriptase (Life technologies) was then added and each cell was incubated overnight at 42 °C in a total volume of 10 μl. To verify the absence of contamination by non-muscular mRNA, samples of bath solution were reverse transcribed. Negative controls where reverse transcriptase was omitted were also included. The cDNA was stored at −80 °C until used for PCR analysis. Optimization of the PCR conditions, such as primer combinations, $MgCl_2$ concentration, number of cycles and annealing temperature were determined using serial dilutions of cDNA from mouse brain and muscle tissues. The conditions that were chosen yielded specific PCR products from 50×10^{-12} g RNA after two rounds of PCR. First and nested primer pairs were intron overspanning. In a single-fibre sample, cDNA of the α_{1G} and α_{1H} subunits were co-amplified along with skeletal muscle α-actin cDNA as a skeletal muscle fibre marker. A first multiplex PCR was performed in a final volume of 50 μl containing 100 nM of each sense and antisense primer, 5 μl RT reaction, 1.25 units of hot-start *Taq* polymerase (Qiagen) and 1 × PCR buffer, using an MJ Research DNA engine. Samples were incubated for 15 min at 94 °C, followed by 20 cycles (94 °C for 30 s, 61 °C for 35 s, 72 °C for 40 s) and a final elongation at 72 °C for 10 min. In the second round of PCR, each transcript was amplified individually using nested primers for α_{1G} and α_{1H} and the same primer pair as in the first PCR for α-actin. The reaction mix included 1 μl of the first PCR product in a final volume of 50 μl containing 50 μM of each dNTP, 100 nM of sense and antisense primer, 1.25 units of hot-start *Taq* polymerase (Qiagen) and 1 × PCR buffer. The $MgCl_2$ concentration in the PCR buffer was 1.5 mM for α_{1G} and α-actin and was increased to 3 mM for amplification of the α_{1H} subunit. Amplification of the α_{1G} subunit was carried out as follows: 94 °C for 15 min, followed by 45 cycles (94 °C for 30 s, 53 °C for 40 s, 72 °C for 40 s) and a final elongation at 72 °C for 10 min. For α_{1H} and α-actin, the PCR protocol included 94 °C for 15 min, followed by 40 cycles (94 °C, 30 s; 55 °C, 40 s; 72 °C, 40 s) and a final elongation at 72 °C for 10 min. Primer sequences, from the 5′ to the 3′ end, and their locations were as follows:

for α_{1G} (GenBank accession number: NM_009783), first,

ACCCTCACCACCTTCAACATCC (position: 1960–1981),
and AATGTGTCGCAGATCAGCCTCC (2294–2315),
and nested, TTCAGCTCCATGCACAAGCTC (1993−2013),
and GCACAGAACTAGGCTCTGCATC (2263–2284);

for α_{1H} (GenBank accession number: AF226868), first,

AGGGGAAGGGCAGCACGG (3161–3178),
and TGCAGGCGGAAGCAGCAG (3441−58),
and nested, CAAGTTCCGTGACTGCAAC (3330–3348),
and GCAGCAGCTATCTTCTATGTC (3427–3447);

for α-actin (GenBank accession number: M12866.1),

CGCGACATCAAAGAGAAGCT (684–703),
and GGGCGATGATCTTGATCTTC (1031–1050)

(Peuker & Pette, 1995). Primers were synthesized by Life technologies.

PCR product analysis

The specificity of the amplification products was verified either by sequencing or restriction digest analysis (results not shown). Amplified DNA fragments were electrophoresed on a 1.5 % (tissue RT-PCR) or 2.5 % (single-fibre RT-PCR) agarose gel containing ethidium bromide, in parallel with a molecular ruler (1 kb DNA ladder, Life technologies or 100 bp PCR ladder, Sigma).

RESULTS

In 100 % of the studied myofibres isolated from mouse fetuses, depolarizing pulses from a holding potential of −80 mV evoked a low threshold, transient (T-type) Ca^{2+} current and a high threshold, sustained (L-type) Ca^{2+} current. The application of a 750 ms duration prepulse to −30 mV inactivated the T-type current (see Strube *et al.*

2000). Subtraction of the recordings obtained with prepulse from those obtained without prepulse allowed us to isolate the T-type Ca^{2+} current. We were also able to isolate the T-type current by blocking the L-type current with the addition of 5 μM nifedipine in the bath. The results obtained by the two methods were comparable, but in presence of nifedipine the pipette seal was unstable. Thus, although the subtraction method is tedious due to the large number of recordings it requires, this method was chosen to generate all the results presented here. Figure 1*A* shows a typical family of current traces in response to a set of depolarizing pulses obtained after subtraction. Activation and inactivation were slow near threshold and accelerated with increasing depolarization, producing the criss-crossing pattern characteristic of the T-type current. Such recordings obtained at different stages of prenatal development allowed us to study the voltage dependence of the T-type current during prenatal myogenesis.

Figure 1*B* shows the voltage dependence of the peak current density at E14, E15, E16, E17 and E18. Detectable currents appeared at approximately −45 mV and the maximum density was observed at approximately −15 mV for all prenatal stages. The current density depended on the developmental stage with the largest density recorded in myofibres from 16-day-old fetuses. The fit of these *I–V*

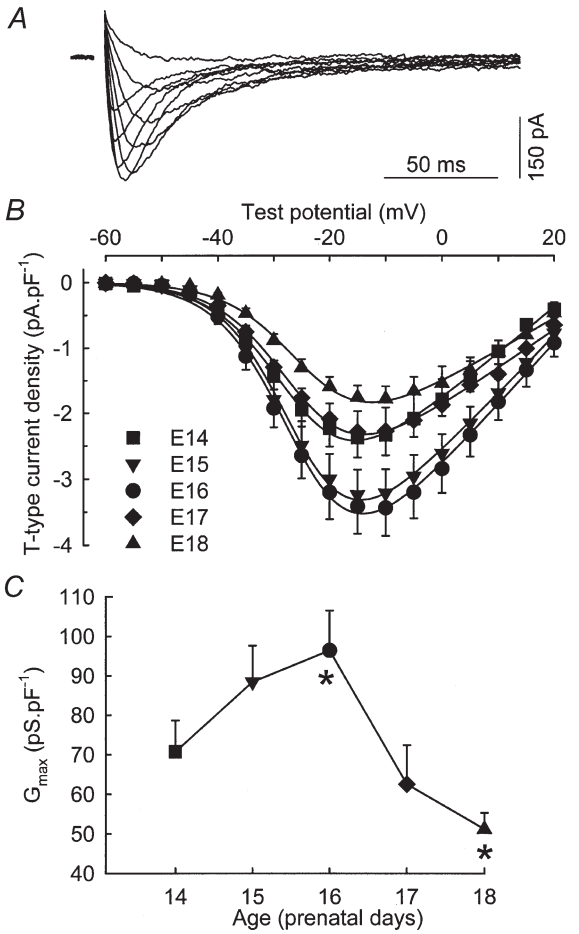

Figure 1. Voltage dependence of T-type Ca^{2+} current density during prenatal myogenesis

A, superimposition of difference traces, in response to test pulses to −45, −40, −35, −30, −25, −15, −5, 5 and 15 mV. The cell was isolated from a fetus at E16 and had a capacitance of 187 pF. *B*, voltage dependence of the average density of T-type Ca^{2+} current recorded in myofibres from 14- (n = 13), 15- (n = 10), 16- (n = 15), 17- (n = 8) and 18-day-old (n = 8) fetuses. The curves correspond to a fit to the mean data at each age using eqn (1) from Methods. *C*, average maximum macroscopic conductance calculated from the *I–V* curve as described in Methods plotted *versus* the age of the fetuses. Asterisks indicate two values which are significantly different (ANOVA test, $P < 0.05$).

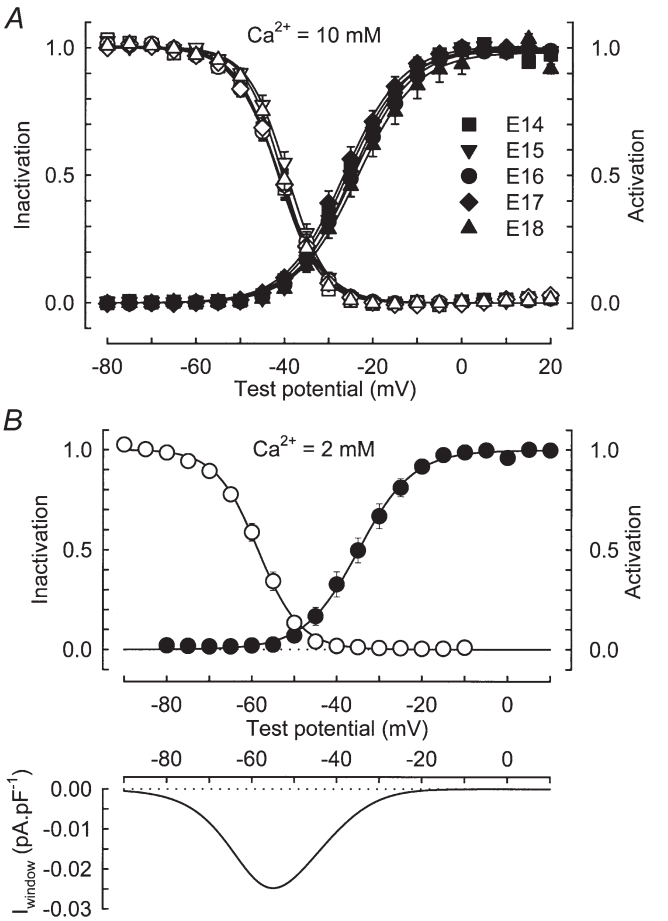

Figure 2. Properties of the T-type Ca^{2+} current during prenatal myogenesis

A, voltage dependence of T-type Ca^{2+} current activation (filled symbols) and inactivation (open symbols) in myofibres from 14- (n = 13), 15- (n = 10), 16- (n = 15), 17- (n = 8) and 18-day-old (n = 8) fetuses in the presence of 10 mM external Ca^{2+}. The data for the activation and inactivation in each cell were obtained as described in Methods and then averaged on this graph. Continuous lines correspond to a Boltzmann fit to the population average. *B*, top, same curves as in *A* but in the presence of 2 mM external Ca^{2+}. The data were obtained from 9 cells at E16. Parameters of the fits are $V_{½,ac}$ = −34.8 mV, k_{ac} = 6.36 mV, $V_{½,inac}$ = −58.6 mV and k_{inac} = −5.00 mV. Bottom, putative window current obtained by multiplying the predicted peak current–voltage curve by the predicted steady-state inactivation curve. The average window current reached a maximum of 0.025 pA pF^{-1} at a potential of −54.8 mV.

Table 1. Variation of some biophysical parameters characteristic of T-type Ca^{2+} current during prenatal myogenesis

	E14	E15	E16	E17	E18
G_{max} (pS pF^{-1})	70.7 ± 7.9	88.4 ± 9.2	96.4 ± 10.1	62.5 ± 9.9	51.2 ± 4.1
I_{max} (pA pF^{-1})	−2.45 ± 0.31	−3.26 ± 0.38	−3.58 ± 0.43	−2.39 ± 0.38	−1.85 ± 0.19
V_{rev} (mV)	24.4 ± 1.3	27.7 ± 1.0	28.9 ± 2.1	29.5 ± 1.8	29.4 ± 2.7
$V_{½,ac}$ (mV)	−25.8 ± 0.9	−24.8 ± 1.1	−24.3 ± 0.9	−26.5 ± 1.4	−22.9 ± 1.6
k_{ac} (mV)	6.33 ± 0.18	5.97 ± 0.18	6.41 ± 0.15	6.12 ± 0.12	6.74 ± 0.45
$V_{½,inac}$ (mV)	−41.4 ± 0.8	−39.4 ± 0.8	−41.1 ± 0.9	−41.1 ± 1.1	−40.6 ± 0.7
k_{inac} (mV)	−4.31 ± 0.16	−4.20 ± 0.11	−4.69 ± 0.15	−4.58 ± 0.15	−4.13 ± 0.25
t_{peak} (ms)	13.0 ± 0.5	12.8 ± 1.0	11.5 ± 0.4	12.0 ± 0.5	12.1 ± 0.5
No. of cells	13	10	15	8	8

G_{max}, V_{rev}, $V_{½,ac}$, k_{ac}, $V_{½,inac}$ and k_{inac} are calculated as described in Methods. I_{max} is the maximum density of T-type current determined from the fit of the *I–V* curve. t_{peak} is the duration between the beginning of the pulse and the peak amplitude of the T-type current for a depolarization reaching −10 mV. The mean values (± S.E.M.) given here are calculated by averaging the parameters determined by the fits to each cell data. The values of the different parameters obtained by fitting the average data (as done for the smooth curves shown in Figs 2 and 3) are always included within the error bars given here.

curves with eqn (1) described in Methods allowed us to determine, as a function of age, the maximum macroscopic conductance (G_{max}), the apparent reversal potential (V_{rev}) and the maximum density of current (I_{max}). In agreement with our previous results (Shimahara & Bournaud, 1991; Strube *et al.* 2000), G_{max} and I_{max} increased and then decreased in cells from 14- to 18-day-old fetuses (Fig. 1*C* and Table 1), with a peak at E16 (I_{max}, ~3.5 pA pF^{-1}) and significantly smaller values at E14 (I_{max}, ~2.4 pA pF^{-1}) and E18 (I_{max}, ~1.8 pA pF^{-1}). In contrast, V_{rev} did not significantly change during the same period, suggesting that the selectivity of the channel for Ca^{2+} was not altered.

The voltage dependence of activation is clearly visualized in Fig. 2*A* where it is reported together with the voltage dependence of inactivation of the T-type current for the various stages studied. The main observation is that there was no significant change of either the activation or the

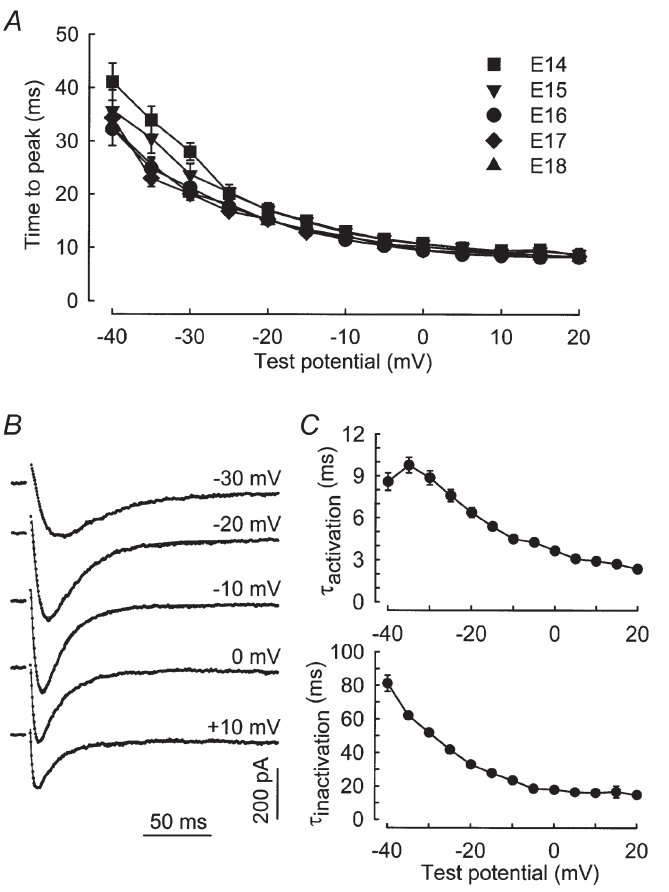

Figure 3. Kinetics of the T-type Ca^{2+} current

A, voltage dependence of the time to peak in myofibres from 14- (n = 13), 15- (n = 10), 16- (n = 15), 17- (n = 8) and 18-day-old (n = 8) fetuses. *B*, T-type Ca^{2+} current evoked in response to test depolarizations from a holding potential of −80 mV to the indicated potentials. The continuous lines correspond to a fit to the experimental data using eqn (3) described in Methods. Capacitance of the cell isolated from a 16-day-old fetus was 111.5 pF. *C*, voltage dependence of the activation (top) and inactivation (bottom) time constants of the T-type Ca^{2+} current. Values are means ± S.E.M. of 20 cells at E16.

inactivation curves over the studied period. This result was confirmed by the average values of $V_{½,ac}$, k_{ac}, $V_{½,inac}$ and k_{inac} given in Table 1 which summarizes the mean values (± S.E.M.) of each parameter at each developmental stage. At all stages, we observed a window current characterized by an overlap of the activation and inactivation curves, which was centred at about −34 mV.

To evaluate the range of potentials in which the T-type Ca^{2+} current might contribute to skeletal muscle function, a series of experiments using 2 mM rather than 10 mM external Ca^{2+} were performed. Moreover, a 10 s conditioning pulse was used to construct the inactivation curve in order to reach the steady-state inactivation and thus to determine the putative window current. Figure 2*B* (top) gives the average voltage dependence of activation and inactivation of T-type current in fibres from 16-day-old fetuses ($n = 9$). In the presence of 2 mM external Ca^{2+}, the maximum conductance was three times smaller than in 10 mM Ca^{2+} (30.0 ± 3.5 pS pF^{-1} *vs.* 96.4 ± 10.1 pS pF^{-1}). The half-activation potential was −33.7 ± 1.8 mV, whereas half-steady-state inactivation occurred at −57.9 ± 1.1 mV, values which are shifted towards more negative potentials relative to those obtained in the presence of 10 mM Ca^{2+} (see Table 1 for comparison). Computation of the voltage dependence of activation and inactivation evaluated in each of the nine myotubes revealed that a maximum window current was generated at a potential of −53.5 ± 0.7 mV and that its amplitude amounted to 0.022 ± 0.003 pA pF^{-1} (average curve shown in Fig. 2*B*, bottom).

Regarding the activation and inactivation kinetics, the time to peak (time from the start of the pulse to the peak of the current) displayed the same voltage dependence at all studied stages (Fig. 3*A*). For potentials more depolarized than −10 mV, the time to peak for the recorded T-type current varied between 10 and 15 ms (Table 1). For potentials more negative than −30 mV, the time to peak was slightly slower in myofibres from the E14 and E15 stages than in myofibres from older fetuses. The T-type current traces could be fitted by the sum of two exponential components, as described in Methods (eqn (3), Fig. 3*B*). Activation and inactivation kinetics were voltage dependent, both accelerating with depolarization and hardly reaching steady state at about 3 and 16 ms for membrane potentials above 5 and −5 mV, respectively (Fig. 3*C*).

Figure 4 illustrates the characteristics of the recovery from inactivation of T-type current recorded in myofibres from 16-day-old fetuses. The time dependence of reactivation from short-term inactivation was studied with a repetitive pulse protocol, where inactivation was induced by a 250 ms depolarization to −20 mV and relieved by a

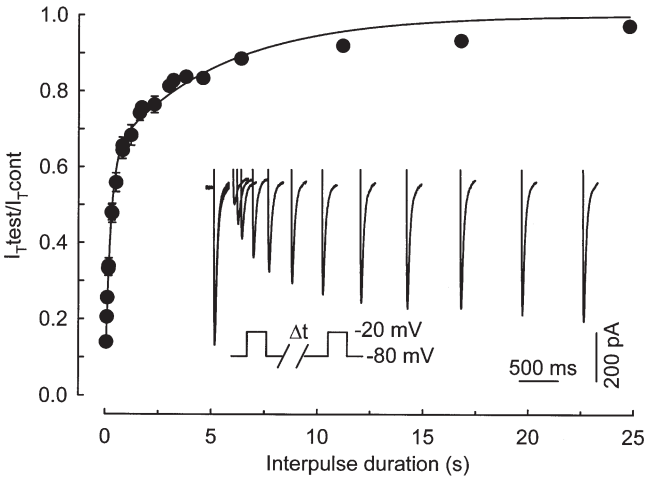

Figure 4. Time dependence of recovery from short-term inactivation

Average plots (from 12 cells at E16) of the relative peak current elicited by the test pulse as a function of the interpulse duration. The relationship was fitted by a double exponential with a time constant of 224 ms for 63 % of the current and 5.16 s for the other 37 % of the current. Inset, superimposed current traces from the beginning of a typical experiment showing the increase of the current induced by the test pulse when the recovery interval grew longer. The time dependence of recovery was studied using a paired pulse protocol (see below the traces) applied every 60 s and where inactivation was induced by a 250 ms depolarization to −20 mV. Capacitance of the cell isolated from a 16-day-old fetus was 302 pF.

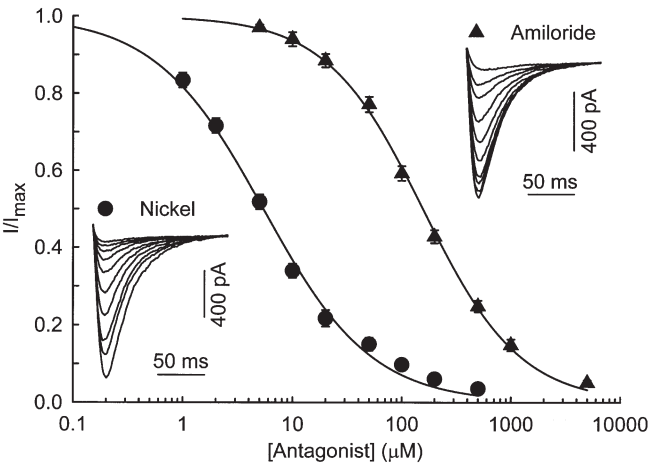

Figure 5. Effect of nickel ions and amiloride on T-type Ca^{2+} current

Dose–response curve for the block of T-type Ca^{2+} current by the antagonist. Data represent the average (± S.E.M.) responses from 9 and 7 cells at E16, for $NiCl_2$ and amiloride, respectively. The smooth curves represent the fit of the Hill equation to the data with IC_{50} = 5.4 and 156 μM and n_H = 0.88 and 0.98 for $NiCl_2$ and amiloride, respectively. Insets, typical responses to increasing concentrations of $NiCl_2$ and amiloride. Test pulses to −20 mV from a holding potential of −80 mV were delivered every 20 s. Traces shown here are control traces and current in presence of 1, 2, 5, 10, 20, 50, 100, 200 and 500 μM $NiCl_2$ or 5, 10, 20, 50, 100, 200, 500, 1000 and 5000 μM amiloride. Capacitance of the cells isolated from 16-day-old fetuses was 152 and 109 pF, respectively.

repolarization of variable duration at −80 mV. The paired pulse protocol was applied every 60 s. The current induced by the second test pulse grew larger when the recovery interval increased (Fig. 4, inset). The fractional recovery, calculated as the ratio of the peak current elicited by the second depolarizing pulse to the peak current during the conditioning pulse, is plotted as a function of the interpulse duration. The relationship was best fitted by the sum of two exponential functions, which suggests a reactivation time course occurring in two separate phases. Approximately 65 % of the current recovered from inactivation with a time constant of 224 ms and the remaining 35 % with a time constant of 5160 ms. Comparable values were obtained at E18 (data not shown).

The last characteristic we studied was the sensitivity of the T-type Ca^{2+} current to $NiCl_2$ and amiloride (Fig. 5). To determine the dose dependence of the drug block, several concentrations of antagonists were applied sequentially, and their effect was measured every 20 s by a test pulse to −20 mV from a holding potential of −80 mV. Representative traces of a typical experiment are shown in Fig. 5. The left inset shows control recording and representative recordings obtained in presence of 1, 2, 5, 10, 20, 50, 100, 200 and 500 μM $NiCl_2$ (from the largest to the smallest current). The right inset is similar but with concentrations of amiloride of 5, 10, 20, 50, 100, 200, 500, 1000 and 5000 μM. The T-type current was significantly blocked by low micromolar concentrations of $NiCl_2$ but higher concentrations of amiloride were required to produced the same blocking effect. The block was almost complete at a concentration of 500 μM $NiCl_2$ and 5 mM amiloride. The nickel block was fully reversible in approximately 5 min but the recovery after the application of 5 mM amiloride was never complete. However, the application of 1 mM amiloride was totally reversible in less than 5 min. The application of antagonist (either amiloride or $NiCl_2$) did not change the kinetics of the current except in the case of application of 5 mM of amiloride, which delayed the time to peak by about 20 %, as already described by Lacinova *et al.* (2000*a*). Figure 5 shows the average dose–response curve obtained from nine cells in the presence of $NiCl_2$ and seven cells with amiloride. Data were fitted with a single Hill function as described in Methods. The Hill slope was close to 1, and the concentrations of antagonist at which half of the T-type current was blocked (IC_{50}) were 5.4 μM for $NiCl_2$ and 156 μM for amiloride, revealing a high sensitivity of the current to $NiCl_2$.

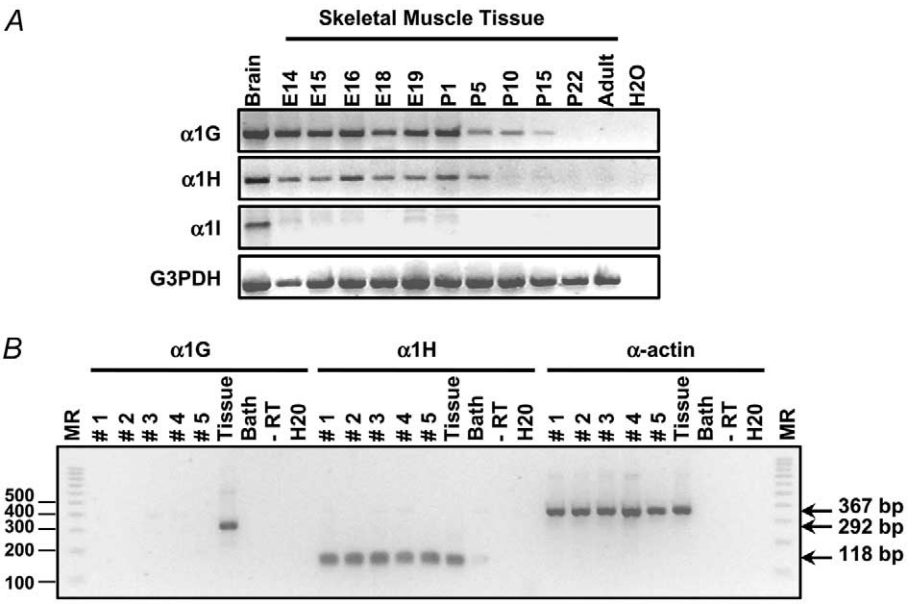

Figure 6. Expression of the mRNAs corresponding to the α_{1G}, α_{1H} and α_{1I} T-type Ca^{2+} channel subunits during skeletal muscle development

A, α_{1G}, α_{1H} and α_{1I} transcripts were detected by RT-PCR in muscle tissue samples from various embryonic (E) and postnatal (P) stages and from adult mouse using specific forward and reverse primers as described in Methods. Brain sample was used as a positive control and water as a negative control. G3PDH amplification was performed on all samples as a positive control. *B*, single-fibre RT-PCR analysis on isolated fibres from 18-day-old fetuses. Expression of α_{1G}, α_{1H} and skeletal muscle α-actin transcripts was analysed on five different fibres (lanes numbered 1 to 5) and on 50×10^{-12} g of RNA from whole skeletal muscle tissue (lane 'Tissue'). Note that PCR products corresponding to α_{1H} (118 bp) and α-actin (367 bp) transcripts are present in all analysed fibres and in whole muscle tissue whereas the PCR product corresponding to the α_{1G} subunit transcript (292 bp) is only detected in muscle tissue. Negative controls are the corresponding bath solution, a single-fibre sample without reverse transcriptase and water. The size of the different fragments in the molecular ruler (MR, 100 bp PCR ladder) is shown on the left.

To determine the molecular origin of the skeletal muscle T-type channels, we performed RT-PCR analysis on skeletal muscle tissues collected at various stages of development, from prenatal to adult. As shown in Fig. 6*A*, α_{1I} mRNA was not detectable at any stage. In contrast, mRNA encoding the α_{1G} and α_{1H} subunits were present at all prenatal stages. These transcripts disappeared after 2 and 3 weeks, for α_{1H} and α_{1G}, respectively. The expression of these transcripts was also analysed at the single-cell level by RT-PCR analysis on freshly dissociated fibres from 18-day-old fetuses. At this stage, skeletal muscle fibres were large enough to be separated from other cell types by filtering. Also, the current density at this stage was still appreciable and all the other characteristics of the T-type channel were similar to those of the other stages studied. Figure 6*B* shows representative results of a multiplex RT-PCR analysis where each single fibre was tested simultaneously for expression of the α_{1G} and α_{1H} subunit mRNAs and the skeletal muscle α-actin mRNA. Most single-fibre RT-PCR samples (10 of 12) yielded a specific PCR product for the α-actin gene, indicating a good efficiency of mRNA harvesting and reverse transcription. Samples where the α-actin gene could not be amplified did not either yield to amplification of α_1 mRNAs, thus suggesting that these negative results were probably due to cell loss. In the α-actin-positive single-fibre samples, mRNA encoding the α_{1G} subunit was not detected whereas α_{1H} mRNA was always present. The high sensitivity of the single-cell RT-PCR technique could lead to false-positive results even when minimal contamination from non-skeletal muscle fibre mRNA occurs. As a control, samples of bath solution aspirated next to the single fibres were also analysed by RT-PCR. They did not yield positive signals, thus demonstrating that the care taken to filter and wash the isolated fibres suspension prevented any contamination. Moreover, the absence of RT-PCR signals in single-fibre samples where RT was omitted showed that genomic DNA could not be amplified in our assay. In contrast, using RT-PCR conditions identical to those in the assays on single-fibres, both α_{1G} and α_{1H} mRNAs were detected in control samples of whole muscle tissue using 50×10^{-12} g RNA, which corresponds to the amount of total RNA estimated to be contained in a single muscle fibre. Single-fibre RT-PCR analysis thus strongly suggested that skeletal muscle fibres express the α_{1H} but not the α_{1G} subunit at day 18 of fetal life and that the product corresponding to the α_{1G} subunit detected by RT-PCR from muscle tissue samples is likely to originate from cells of non-skeletal muscle origin.

DISCUSSION

In the present work, we have characterized in detail the electrophysiological properties of the T-type Ca^{2+} current during prenatal myogenesis in mouse skeletal muscle, and we provide molecular, electrophysiological and pharmacological evidence that these channels are generated by the functional expression of the α_{1H} subunit. The transient expression of the T-type α_{1H} channels described in this work correlates well with critical events relevant to skeletal muscle physiology and taking place during prenatal period, such as myoblast fusion and other early differentiation steps that require gene activation and intracellular calcium regulation. Additionally, the properties of the T-type channels in freshly isolated mouse skeletal muscle fibres correspond well with those of cultured human fusion-competent myoblasts in which antisense against α_{1H} mRNA reduced T-type Ca^{2+} conductance and myoblast fusion (Bijlenga *et al.* 2000). Overall, our results are consistent with the notion that the T-type channel is critical for skeletal muscle development events and that its expression is regulated by a process associated with skeletal muscle differentiation.

An important finding of our study is that the electrophysiological properties of the T-type channels in freshly isolated mouse embryonic skeletal muscle fibres are constant throughout prenatal life, and thus, can be compared with those of cloned channels. All three cloned T-type channels expressed in oocytes or in HEK 293 cells display largely similar properties (Perez-Reyes, 1999). However, the α_{1I} subunit can be distinguished from α_{1G} and α_{1H} by slower activation and inactivation kinetics (Klöckner *et al.* 1999; Kozlov *et al.* 1999; Monteil *et al.* 2000*b*). The time constant of activation of the mouse skeletal T-type current (< 5 ms for potentials above -10 mV) and the time constant of inactivation ($\sim$16 ms for potentials above -5 mV) were similar to those calculated for the channels generated by α_{1G} and α_{1H} expressed in HEK 293 cells (Klöckner *et al.* 1999; Kozlov *et al.* 1999; Williams *et al.* 1999; Monteil *et al.* 2000*b*). In addition, the α_{1H} current can be distinguished from the α_{1G} and α_{1I} currents by its higher sensitivity to nickel ions (Lee *et al.* 1999*b*) and to amiloride (Lacinova *et al.* 2000*b*). The IC_{50} value of 5.4 μM determined for the block of the mouse skeletal muscle T-type current by nickel ions in our experiments revealed a high sensitivity to Ni^{2+} similar to the one determined for α_{1H} channels expressed in oocytes by Lee *et al.* (5.7 μM, 1999*b*) and in HEK 293 cells by Williams *et al.* (6.6 μM, 1999). In contrast, it is much lower than the IC_{50} determined in HEK 293 cells for α_{1G} (250 μM, Lee *et al.* 1999*b* and 133 μM, Monteil *et al.* 2000*b*) and for α_{1I} (216 μM, Lee *et al.* 1999*b* and 184 μM, Monteil *et al.* 2000*b*). Concerning amiloride, the IC_{50} of 156 μM determined in our experiments is clearly similar to that determined for the human α_{1H} channel expressed in HEK 293 (167 μM, Williams *et al.* 1999), whereas the murine α_{1G} channel expressed in HEK 293 is more than 30 times less sensitive to amiloride (Lacinova *et al.* 2000*a*). According to these distinctive biophysical and pharmacological properties of the cloned α_{1G}, α_{1H} and α_{1I} subunits when expressed in heterologous systems, our data indicate that T-type currents in mouse fetal skeletal

fibres correspond to channels generated by the α_{1H} subunit.

The RT-PCR analysis of prenatal skeletal whole muscle and single fibres showed that mRNAs corresponding to the α_{1G} and α_{1I} subunits are absent, whereas mRNA for the α_{1H} subunit is present at this stage of development. These results are in good agreement with the electrophysiological data that suggested that the α_{1G} and α_{1I} subunits were unlikely to generate skeletal muscle T-type currents. It should be noted however that in whole muscle tissue both α_{1G} and α_{1H} mRNAs were detected. Because whole muscle is not solely constituted of muscle fibres, but also consists of fibroblasts, vascular smooth muscle cells and nerves, it can be hypothesized that the α_{1G} transcript is associated with non-skeletal muscle cell types that express a large amount of α_{1G} subunit at the fetal stage (Monteil *et al.* 2000*a*). Thus, considering muscle tissue heterogeneity, single-fibre RT-PCR proved to be the most appropriate method for studying the expression pattern of T-type channel transcripts in skeletal muscle cells in association with cellular electrophysiological characteristics. Yet, it is important to note that expression of α_{1G} subunit mRNA appears to be developmentally regulated in whole muscle tissue, rapidly declining and becoming undetectable 3 weeks after birth. This observation suggests that the α_{1G} subunit could play a role in the development of muscle tissue and will certainly justify further investigations, starting with the localization of the protein.

Although our results clearly demonstrate that α_{1H} subunit gene is the one encoding the T-type channel expressed in skeletal muscle fibres during development, a careful comparison of the properties of the current recorded in skeletal muscle and in heterologous systems expressing α_{1H} reveals some differences. The recovery from short-term inactivation in skeletal muscle cells occurred with a very slow time constant (more than 5 s for the slower component) which is longer than those described for the three cloned α_1 subunits responsible for T-type channels stably transfected in HEK 293. Studying α_{1H} recovery from short-term inactivation with protocols similar to ours, J. Hering & R. C. Lambert (personal communication) and Klöckner *et al.* (1999) obtained recovery time constant values smaller than 1 s. Even though the results may be protocol related, such a difference can hardly be explained only by a lower Ca^{2+} concentration (1.5 mM and 2.5 mM *versus* 10 mM) and a smaller interpulse interval (8 s versus 60 s). Also, the activation and inactivation kinetics determined in presence of 10 mM Ca^{2+} in our myofibres and in HEK 293 cells by Klöckner *et al.* (1999) are slightly different. For depolarizations above −20 mV, the activation is slower and the inactivation is faster in myotubes than in HEK 293 cells. Altogether these results suggest that the expression of α_{1H} in developing muscle could be modulated by some factors absent in heterologous systems, such as auxiliary α_2/δ (Dolphin *et al.* 1999) or γ (Klugbauer *et al.* 2000) subunits, and/or muscle-specific proteins, and/or degree of phosphorylation. The difference of expression pattern could also be due to the expression of specific splice variants, as already seen with the expression of α_{1G} (Chemin *et al.* 2001).

In agreement with previous work (Shimahara & Bournaud, 1991; Strube *et al.* 2000), we show here that the T-type Ca^{2+} current undergoes a transient expression during myogenesis. The maximum macroscopic conductance increases to reach a maximum (96.4 ± 10.1 pS pF^{-1} in 10 mM Ca^{2+}) at E16 and then decreases until birth. Gonoi & Hasegawa (1988) showed that the T-type current continues to decrease after birth and becomes undetectable at about 2 weeks after birth. This regulated expression of the T-type current in a development-dependent fashion is in good agreement with our RT-PCR results and suggests that this current could play a specific role during skeletal muscle maturation. In 10 mM external Ca^{2+}, the threshold of activation is around −45 mV and the window current is centred on −34 mV. Under the same conditions, L-type current is activated above −20 mV (Strube *et al.* 2000), and the threshold for the intracellular Ca^{2+} transients is above −30 mV (Strube *et al.* 1996). Thus, the T-type channel allows Ca^{2+} entry at potentials more negative than the L-type channel. In more physiological conditions ($[Ca^{2+}]_E$ = 2 mM, Fig. 2*B*), the activation and inactivation curves are shifted by about 10 mV towards negative potentials and there is a large window current with a peak at about −55 mV. These values are comparable to those described in fusion competent human myoblasts (Bijlenga *et al.* 2000) and about 10 mV more positive than those reported for HEK 293 cells overexpressing the α_{1H} subunit (Chemin *et al.* 2000). Taken together, these results suggest that T-type current would allow Ca^{2+} entry at potentials more negative than those required for contraction threshold and closer to the resting membrane potential. Even though the window current is not centred on the resting potential, a significant amount of Ca^{2+} could enter the cell through the T-type channel because this window in 2 mM Ca^{2+} is broad, starting below −80 mV and ending at about −20 mV. In addition, due to the early stage of development of the studied cells, the resting potential may not be as negative as −80 mV, but closer to the centre of the window current. Thus, in developing muscle fibres, the large window current described here could induce an increase in basal intracellular Ca^{2+} concentration necessary for the fusion process (Bijlenga *et al.* 2000) and/or gene expression (Grinell, 1995). As an emphasis to the possible role of the T-type current in skeletal muscle, it is important to notice that T-type window currents have also been described in developing cardiac cells and decrease in adult cells (Cohen & Lederer, 1988). In skeletal muscle, the presence of T-type channel activity during prenatal

myogenesis is concomitant with two important events. One is the formation of primary muscle fibres, as a consequence of embryonic myoblasts fusion, which begins at about E13. The second is the appearance of secondary muscle fibres, resulting from the fetal myoblasts fusion, which takes place at about E16. Giving the time course of current expression (Fig. 1*C*), the T-type channel is more likely to contribute to the latter rather than the former process.

The unique electrophysiological characteristics of the T-type Ca^{2+} current recorded here in native skeletal muscle and the fine-tuned developmental regulation of the corresponding T-type Ca^{2+} channel, encoded by the CACNA1H gene which produces the α_{1H} ($Ca_V3.2$) subunit, provide further support to the hypothesis that this low voltage activated Ca^{2+} current plays a major role not only in muscle regeneration but also in embryonic muscle formation. Further investigations are needed to determine the precise physiological relevance of T-type channel activity in developing skeletal muscle *in vivo*.

REFERENCES

Beam, K. G. & Knudson, C. M. (1988*a*). Calcium currents in embryonic and neonatal mammalian skeletal muscle. *Journal of General Physiology* **91**, 781–798.

Beam, K. G. & Knudson, C. M. (1988*b*). Effect of postnatal development on calcium currents and slow charge movement in mammalian skeletal muscle. *Journal of General Physiology* **91**, 799–815.

Bijlenga, P., Liu, J.-H., Espinos, E., Haenggli, C.-A, Fischer-Lougheed, J., Bader, C. R. & Bernheim, L. (2000). T-type alpha1H Ca^{2+} channels are involved in Ca^{2+} signaling during terminal differentiation (fusion) of human myoblasts. *Proceedings of the National Academy of Sciences of the USA* **97**, 7627–7632.

Bossu, J.-L., Feltz, A. & Thomann, J. M. (1985). Depolarization elicits two distinct calcium currents in vertebrate sensory neurones. *Pflügers Archiv* **403**, 360–368.

Carbone, E. & Lux, H. D. (1984). A low voltage-activated, fully inactivating Ca channel in vertebrate sensory neurones. *Nature* **310**, 501–502.

Catterall, W. A. (1991). Excitation-contraction coupling in vertebrate skeletal muscle: a tale of two calcium channels. *Cell* **64**, 871–874.

Chemin, J., Monteil, A., Bourinet, E., Nargeot, J. & Lory, P. (2001). Alternatively spliced alpha1G (CaV3.1) intracellular loops promotes specific T-type calcium channel gating properties. *Biophysical Journal* **80**, 1238–1250.

Chemin, J., Monteil, A., Briquaire, C., Richard, S., Perez-Reyes, E., Nargeot, J. & Lory, P. (2000). Overexpression of T-type calcium channels in HEK-293 cells increases intracellular calcium without affecting cellular proliferation. *FEBS Letters* **478**, 166–172.

Chomczynski, P. & Sacchi, N. (1987). Single-step method of RNA isolation by acid guanidinium thiocyanate-phenol-chloroform extraction. *Analytical Biochemistry* **162**, 156–159.

Cognard, C., Lazdunski, M. & Romey, G. (1986). Different types of Ca^{2+} channels in mammalian skeletal muscle cells in culture. *Proceedings of the National Academy of Sciences of the USA* **83**, 517–521.

Cohen, N. M. & Lederer, W. J. (1988). Changes in the calcium current of rat heart ventricular myocytes during development. *Journal of Physiology* **406**, 115–146.

Cribbs, L. L., Lee, J. H., Satin, J., Zhang, Y., Daud, A., Barclay, J., Williamson, M. P., Fox, M., Rees, M. & Perez-Reyes, E. (1998). Cloning and characterization of alpha1H from human heart, a member of the T-type Ca^{2+} channel gene family. *Circulation Research* **83**, 103–109.

Dolphin, A. C., Wyatt, C. N., Richards, J., Beattie, R. E., Craig, P., Lee, J.-H., Cribbs, L. L., Volsen, S. G. & Perez-Reyes, E. (1999). The effect of α2-δ and other accessory subunits on expression and properties of the calcium channel α1G. *Journal of Physiology* **519**, 35–45.

Gonoi, T. & Hasegawa, S. (1988). Post-natal disappearance of transient calcium channels in mouse skeletal muscle: effects of denervation and culture. *Journal of Physiology* **401**, 617–637.

Grinnell, A. D. (1995). Dynamics of nerve-muscle interaction in developing and mature neuromuscular junctions. *Physiological Reviews* **75**, 789–834.

Hagiwara, S., Ozawa, S. & Sand, O. (1975). Voltage clamp analysis of two inward current mechanisms in the egg cell membrane of a starfish. *Journal of General Physiology* **65**, 617–644.

Klöckner, U., Lee, J. H., Cribbs, L. L., Daud, A., Hescheler, J., Pereverzev, A., Perez-Reyes, E. & Schneider, T. (1999). Comparison of the Ca^{2+} currents induced by expression of three cloned alpha1 subunits, alpha1G, alpha1H and alpha1I, of low-voltage-activated T-type Ca2 + channels. *European Journal of Neuroscience* **11**, 4171–4178.

Klugbauer, N., Dai, S., Specht, V., Lacinova, L., Marais, E., Bohn, G. & Hofmann, F. (2000). A family of gamma-like calcium channel subunits. *FEBS Letters* **470**, 189–197.

Kozlov, A. S., McKenna, F., Lee, J-H., Cribbs, L. L., Perez-Reyes, E., Feltz, A. & Lambert, R. C. (1999). Distinct kinetics of cloned T-type Ca^{2+} channels lead to differential Ca^{2+} entry and frequency-dependence during mock action potentials. *European Journal of Neuroscience* **11**, 4149–4158.

Lacinova, L., Klugbauer, N. & Hofmann, F. (2000*a*). Regulation of the calcium channel alpha1G subunit by divalent cations and organic blockers. *Neuropharmacology* **39**, 1254–1266.

Lacinova, L., Klugbauer, N. & Hofmann, F. (2000*b*). Low voltage activated calcium channels: from genes to function. *General Physiology and Biophysics* **19**, 121–136.

Lambolez, B., Audinat, E., Bochet, P., Crepel, F., & Rossier, J. (1992). AMPA receptor subunits expressed by single Purkinje cells. *Neuron* **9**, 247–258.

Lee, J. H., Daud, A., Cribbs, L. L., Lacerda, A. E., Pereverzev, A., Klöckner, U., Schneider, T. & Perez-Reyes, E. (1999*a*). Cloning and expression of a novel member of the low voltage-activated T-type calcium channel family. *Journal of Neuroscience* **19**, 1912–1921.

Lee, J. H., Gomora, J. C., Cribbs, L. L. & Perez-Reyes, E. (1999*b*). Nickel block of three cloned T-type calcium channels: low concentrations selectively block alpha1H. *Biophysical Journal* **77**, 3034–3042.

Matteson, D. R. & Armstrong, C. M. (1986). Properties of two types of calcium channels in clonal pituitary cells. *Journal of General Physiology* **87**, 161–182.

Melzer, W., Herrmann-Frank, A. & Lüttgau, H. Ch. (1995). The role of Ca^{2+} ions in excitation-contraction coupling of skeletal muscle fibres. *Biochimica et Biophysica Acta* **1241**, 59–116.

Miller, J. B., Schaefer, L. & Dominov, J. A. (1999). Seeking muscle stem cells. *Current Topics in Developmental Biology* **43**, 191–219.

Monteil, A., Chemin, J., Bourinet, E., Mennessier, G., Lory, P. & Nargeot, J. (2000*a*). Molecular and functional properties of the human alpha1G subunit that forms T-type calcium channels. *Journal of Biological Chemistry* **275**, 6090–6100.

Monteil, A., Chemin, J., Leuranguer, V., Altier, C., Mennessier, G., Bourinet, E., Lory, P. & Nargeot, J. (2000*b*). Specific properties of T-type calcium channels generated by the human alpha1I subunit. *Journal of Biological Chemistry* **275**, 16530–16535.

Morris, G. E. & Cole, R. J. (1979). Calcium and the control of muscle-specific creatine kinase accumulation during skeletal muscle differentiation in vitro. *Developmental Biology* **69**, 146–158.

Nilius, B., Hess, P., Lansman, J. B. & Tsien, R. W. (1985). A novel type of cardiac calcium channel in ventricular cells. *Nature* **316**, 443–446.

Nowycky, M. C., Fox, A. P. & Tsien R. W. (1985). Three types of neuronal calcium channel with different calcium agonist sensitivity. *Nature*. **316**, 440–443.

Perez-Reyes, E. (1999). Three for T: molecular analysis of the low voltage-activated calcium channel family. *Cellular and Molecular Life Sciences* **56**, 660–669.

Perez-Reyes, E., Cribbs, L. L., Daud, A., Lacerda, A. E., Barclay, J., Williamson, M. P., Fox, M., Rees, M. & Lee, J. H. (1998). Molecular characterization of a neuronal low-voltage-activated T-type calcium channel. *Nature* **391**, 839–841.

Peuker, H. & Pette, D. (1995). Direct reverse transcriptase-polymerase chain reaction for determining specific mRNA expression levels in muscle fiber fragments. *Analytical Biochemistry* **224**, 443–446.

Salzberg, S., Mandelboim, M., Zalcberg, M., Shainberg, A. & Mandelbaum, M. (1995). Interruption of myogenesis by transforming growth factor beta1 or EGTA inhibits expression and activity of the myogenic-associated (2'-5'). oligoadenylate synthetase and PKR. *Experimental Cell Research* **219**, 223–232.

Seigneurin-Venin, S., Parrish, E., Marty, I., Rieger, F., Romey, G., Villaz, M. & Garcia, L. (1996). Involvement of the dihydropyridine receptor and internal Ca^{2+} stores in myoblast fusion. *Experimental Cell Research* **223**, 301–307.

Shainberg, A., Yagil, G. & Yaffe, D. (1969). Control of myogenesis in vitro by Ca^{2+} concentration in nutritional medium. *Experimental Cell Research* **58**, 163–167.

Shimahara, T. & Bournaud, R. (1991). Barium currents in developing skeletal muscle cells of normal and mutant mice foetuses with 'muscular dysgenesis'. *Cell Calcium* **12**, 727–733.

Strube, C., Beurg, M., Powers, P. A., Gregg, R. G. & Coronado, R. (1996). Reduced Ca^{2+} current, charge movement, and absence of Ca^{2+} transients in skeletal muscle deficient in dihydropyridine receptor beta1 subunit. *Biophysical Journal* **71**, 2531–2543.

Strube, C., Tourneur, Y. & Ojeda, C. (2000). Functional expression of the L-type calcium channel in mice skeletal muscle during prenatal myogenesis. *Biophysical Journal* **78**, 1282–1292.

Williams, M. E., Washburn, M. S., Hans, M., Urrutia, A., Brust, P. F., Prodanovich, P., Harpold, M. M. & Stauderman, K. A. (1999). Structure and functional characterization of a novel human low-voltage activated calcium channel. *Journal of Neurochemistry* **72**, 791–799.

Acknowledgements

We wish to thank Frédérique Cohen-Adad and Etienne Audinat whose advice were critical for the success of single-fibre RT-PCR experiments. We also thank Isabel Ann Lefevre, Lavina Faleiro and Mike Myers for their help in proofreading. This study was supported by the Centre National de la Recherche Scientifique (CNRS), the Université Claude Bernard and by the Association Française contre les Myopathies (AFM). A.M. was supported by Produits Roche (France), GRRC (Groupe de réflexion sur la Recherche Cardio-vasculaire) and AFM.